Journal of Medicinal Chemistry

Article

Grafting Aminocyclopentane Carboxylic Acids onto the RGD Tripeptide Sequence Generates Low Nanomolar αβ/αβ Integrin Dual Binders

Giovanni Casiraghi, Gloria Rassu, Luciana Auzzas, Paola Burreddu, Enrico Gaetani, Lucia Battistini, Franca Zanardi, Claudio Curti, Giuseppe Nicastro, Laura Belvisi, Ilaria Motto, Massimo Castorina, Giuseppe Giannini, and Claudio Pisano

J. Med. Chem., **2005**, 48 (24), 7675-7687• DOI: 10.1021/jm050698x • Publication Date (Web): 04 November 2005

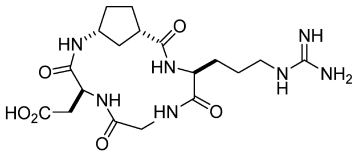

$\alpha_V\beta_3$ IC_{50}: 4.60 nM
$\alpha_V\beta_5$ IC_{50}: 3.43 nM

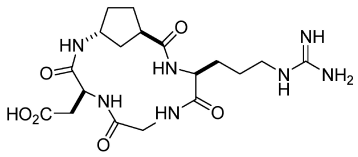

$\alpha_V\beta_3$ IC_{50}: 1.50 nM
$\alpha_V\beta_5$ IC_{50}: 0.59 nM

More About This Article

Additional resources and features associated with this article are available within the HTML version:

- Supporting Information
- Links to the 5 articles that cite this article, as of the time of this article download
- Access to high resolution figures
- Links to articles and content related to this article
- Copyright permission to reproduce figures and/or text from this article

View the Full Text HTML

Journal of Medicinal Chemistry is published by the American Chemical Society. 1155 Sixteenth Street N.W., Washington, DC 20036

Grafting Aminocyclopentane Carboxylic Acids onto the RGD Tripeptide Sequence Generates Low Nanomolar $\alpha_V\beta_3/\alpha_V\beta_5$ Integrin Dual Binders

Giovanni Casiraghi,*,‡ Gloria Rassu,† Luciana Auzzas,† Paola Burreddu,† Enrico Gaetani,‡ Lucia Battistini,‡ Franca Zanardi,‡ Claudio Curti,‡ Giuseppe Nicastro,# Laura Belvisi,§ Ilaria Motto,§ Massimo Castorina,|| Giuseppe Giannini,|| and Claudio Pisano||

Dipartimento Farmaceutico, Università di Parma, Parco Area delle Scienze 27A, I-43100 Parma, Italy, Istituto di Chimica Biomolecolare del CNR, Traversa La Crucca 3, I-07040 Li Punti, Sassari, Italy, Centro Interfacoltà Misure "G. Casnati", Università di Parma, Parco Area delle Scienze 23A, I-43100 Parma, Italy, Dipartimento di Chimica Organica e Industriale, Università di Milano, Via Venezian 21, I-20133 Milano, Italy, and Sigma-Tau, Research & Development, Via Pontina Km 30.400, 00040 Pomezia, Roma, Italy

Received July 21, 2005

Eleven γ-aminocyclopentane carboxylic acid (Acpca) platforms, including four dihydroxy representatives (**19**−**22**), three hydroxy analogues (**34**−**36**), and four deoxy derivatives (**30**−**33**), were prepared in a chiral nonracemic format. These simple units were then grafted onto an Arg-Gly-Asp (RGD) tripeptide framework by a mixed solid phase/solution protocol delivering an ensemble of 11 macrocyclic analogues of type *cyclo*-[-Arg-Gly-Asp-Acpca-], **1**−**11**. The individual compounds were evaluated for their binding affinity toward the $\alpha_V\beta_3$ and $\alpha_V\beta_5$ integrin receptors. The analogue **10** exhibited a very interesting activity profile ($IC_{50}/\alpha_V\beta_3$ = 1.5 nM; $IC_{50}/\alpha_V\beta_5$ = 0.59 nM), comparable to that of reference compounds EMD121974 and ST1646. Closely related congeners **6**, **8**, and **9** also proved to be excellent dual binders with activity levels in the low nanomolar range. The three-dimensional (3D) NMR solution structures were determined, and docking studies to X-ray crystal structure of the extracellular segment of integrin $\alpha_V\beta_3$ in complex with the reference compound EMD121974 were performed on selected analogues to elucidate the interplay between structure and function in these systems and to evidence the subtle bases for receptorial recognition. The results prove that the principle of isosteric dipeptide replacement for peptidomimetics design and synthesis can be violated, without detriment to the development of highly effective integrin binders.

Introduction

In the recent past, small molecular templates that mimic or induce loop and turn secondary structural features of peptides and proteins have gained ample popularity due to the important role they play in molecular recognition and biological events.[1] In particular, great effort is focused on the design and synthesis of a number of molecular platforms encompassing dipeptide core structures,[2] constrained dipeptide surrogates,[3] and nonpeptide motifs,[4] whose incorporation into known peptide sequences has resulted in the creation of promising cyclic and acyclic entities targeting diverse, therapeutically relevant receptors and enzymes. Among the most sought after receptors, the integrin family represents an enterprising biological target,[5] for their diverse components play a prime role in physiopathological processes that span from coagulation of blood,[6] tumor-induced angiogenesis,[7] and control of the immune system[8] to the initiation and progression of tumor metastasis,[9] osteoporosis,[10] restenosis,[11] and inflammatory diseases.[12]

In the present work, we focused on $\alpha_V\beta_3$ and $\alpha_V\beta_5$ integrin receptors, which recognize several matrix proteins through the Arg-Gly-Asp (RGD) tripeptide sequence.[5,13] Today, several major classes and compounds are presented as effective binders of $\alpha_V\beta_3$ and $\alpha_V\beta_5$, where proper inducers of secondary peptide structure are grafted onto the RGD sequence to prevent free rotation of the amide linkages and project peripheral substituents in proper spatial orientations.[2b,3b,7e,14]

The aim of our project was to construct novel macrocyclic, RGD-carrying binders of $\alpha_V\beta_3$ and $\alpha_V\beta_5$ by utilizing hydroxylated and nonhydroxylated γ-aminocyclopentane carboxylic acid (Acpca) platforms that can be seen as γ-aminobutanoic acid (GABA) surrogates locked in a W-conformation by an α,γ-ethylene (or hydroxyethylene) bridge (Figure 1, structure of type **A**).

Although grafting of these small scaffolds onto the RGD consensus motif results in one-atom restriction of the macrocycle size in the formed compounds as compared to previously investigated analogues (14 vs 15 atoms) and violates the classical principle of isosteric dipeptide replacement for peptidomimetics design and synthesis,[15,16] we envisioned that the Acpca motifs would equally provide the requisite scaffolds upon which to design and develop potent integrin ligands for their $\alpha_V\beta_3$ and $\alpha_V\beta_5$ receptors. In other words, we surmised that the global conformational constraint of such chimeric structures arising from the local restriction by the cyclopentane platforms combined with the bias imposed by macrocyclization would result in a favorable spatial orientation of the integrin recognition tripeptide.

* To whom correspondence should be addressed. Phone: +39-0521-905080. Fax: +39-0521-905006. E-mail: giovanni.casiraghi@unipr.it.
‡ Dipartimento Farmaceutico.
† Istituto di Chimica Biomolecolare del CNR.
# Centro Interfacoltà Misure "G. Casnati".
§ Dipartimento di Chimica Organica e Industriale.
|| Sigma-Tau, Research & Development.

10.1021/jm050698x CCC: $30.25
Published on Web 11/04/2005

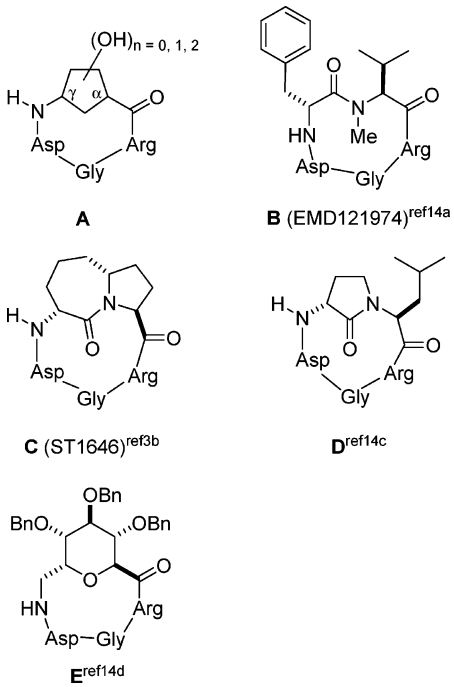

Figure 1. Structural comparison between a generic Acpca-bearing RGD ligand **A** (14-membered cycle) and selected known congeners **B**−**E** (15-membered cycles), highlighting the principle of isosteric dipeptide replacement. As compared to that of the lead cyclopentapeptide **B**, structures of type **C**−**E** satisfy this principle, and the structure of the ring-contracted **A** does not.

The Acpca-containing cyclopeptides **1**−**11** in Figure 2 were synthesized and biochemically evaluated in vitro for their ability to compete with [^{125}I]-echistatin for binding to $\alpha_V\beta_3$ and $\alpha_V\beta_5$ receptors.[17] The influence of the hydroxyl substituents on the cyclopentane units as well as the stereodisposition of peripheral functionality were explored. Finally, to understand the differences in the binding ability for closely related compounds, thorough investigations, including in-solution NMR structural analysis and docking studies of selected analogues to X-ray crystal structure of the extracellular segment of integrin $\alpha_V\beta_3$ in complex with the reference compound EMD121974,[18] were performed.

Results and Discussion

Synthesis of Cyclopentane Amino Acid Building Blocks 19−22 and 30−36. The *N*-Fmoc-protected, dihydroxylated cyclopentane amino acids **19**−**22** utilized to assemble the RGD constructs **1**−**4** were synthesized as enantiomerically pure materials by a modification of our previously reported procedure (Scheme 1).[19] In the first step, silyloxypyrrole **12** was reacted with glyceraldehyde *R*-**13** in diethyl ether under the guidance of $SnCl_4$. The reaction conditions were optimized (slow addition of a 1.0 M solution of $SnCl_4$ in CH_2Cl_2 at −90 °C is critical) to obtain an 82% yield and ≥98% de of unsaturated adduct **14**, which was isolated by simple crystallization of the crude reaction product. Next, the double bond within **14** was saturated and the free hydroxyl group protected as TBS ether. Exposure of this intermediate to ammonium cerium(IV) nitrate in acetonitrile ensured clean removal of the *N*-Boc protection, resulting in the formation of lactam **15** in 87% isolated yield in three steps.

After benzylation of the lactam nitrogen, exposure of the resulting fully protected compound to solid periodic acid in ethyl acetate at room temperature yielded aldehyde **16** directly (89% yield, two steps) via simultaneous deacetonidation and oxidative diol cleavage.[20] The creation of the cyclopentane moiety utilized a highly productive, intramolecular silylative aldol maneuver driven by the Lewis acid−Lewis base reagent system TBSOTf−DIEA, arriving at an isolable 80:20 mixture of two cycloadducts, **17** and **18**, in 98% combined yield. The finale of the synthesis involved four operations (three steps), *N*-debenzylation, hydrolytic fragmentation of the lactam bond with full deprotection, and selective *N*-Fmoc functionalization, yielding individual amino acids **19** and **20** in 89% and 67% yields, respectively. With the optimized conditions in hand, the 10-step synthesis was exactly duplicated to prepare the enantiomerical couple **21** and **22** by simply changing the chirality of the glyceraldehyde precursor, *S*-**13** in lieu of *R*-**13**.

The dideoxy derivatives **30**−**33**, as well as monohydroxylated congeners **34**−**36**, were derived from commercially available sources **23**−**26** and **27**−**29**, respectively, via simple functional group manipulations, as shown in Scheme 2.[21]

All of the components of this precursor collection were prepared as ≥98% pure materials by suitable chromatographic operations and then used to build up our 11-member ensemble of macrocyclic pseudopeptides, **1**−**11**.

Synthesis of Cyclopeptides 1−11. To assemble the targeted 11-component collection of cyclopeptides, **1**−**11**, we first planned to realize linear tetrapeptide precursors of type H-Asp(Bu^t)-Acpca-Arg(Pmc)-Gly-OH and then complete the macrocycle via head-to-tail juncture. The Acpca units, **19**−**22** and **30**−**36**, were critically positioned along the peptide chain, flanked by the aspartate and arginine residues, to create the local constraint that preorganizes the chain terminals toward macrocyclization.[22]

Eleven tetrapeptides of general formula H-Asp(Bu^t)-Acpca-Arg(Pmc)-Gly-OH were synthesized in parallel on solid phase, utilizing a conventional polystyrene-based 2-chlorotrityl chloride resin (Scheme 3). Although this type of linker is quite acid labile, its stability toward bases makes it ideal for the various coupling base promoters as well as for the resident Arg- and Asp-protecting groups using the Fmoc strategy, the product being readily cleaved from the resin under mild acidic conditions (e.g., AcOH in trifluoroethanol).

In the resin-loading step, *N*-Fmoc-glycine was attached to the 2-chlorotrityl linker using a 2.5-fold excess amino acid to ensure maximum yield (≥1.55 mmol/g actual loading). After deprotection of the amino group (20% piperidine in DMF), condensation of the Fmoc-Arg(Pmc)-OH residue was attained using the TBTU−HOBt system in the presence of DIEA. Next, the second amino group within the resin-bound dipeptide Fmoc-Arg(Pmc)-Gly-OcTrt was liberated as usual, and an Acpca platform, chosen among the 11 amino acids of this study (**19**−**22** and **30**−**36**, Schemes 1 and 2), was coupled and the resin-bound tripeptide deprotected.

The Fmoc-Asp(Bu^t)-OH residue was then connected and the amino group liberated to afford a resin-bound tetrapeptide, which was cleaved from the resin with a

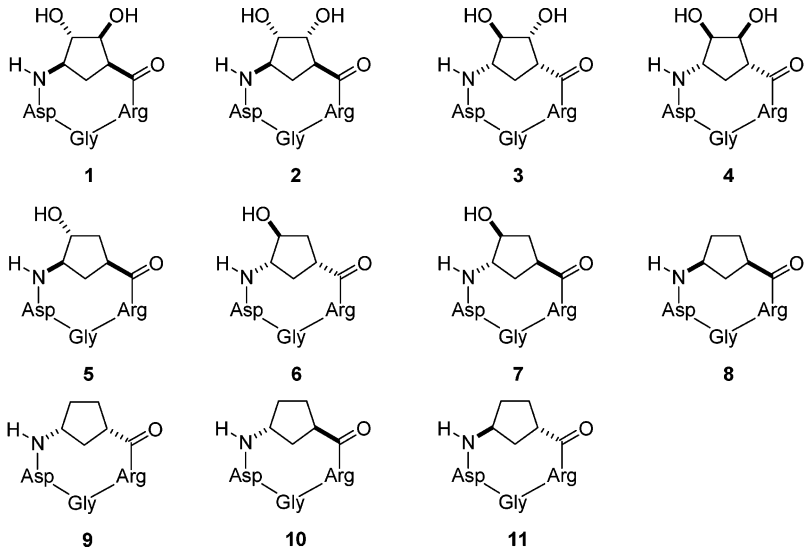

Figure 2. Structures of the targeted RGD-containing cyclopeptides **1**−**11**.

Scheme 1. Synthesis of Dihydroxylated Cyclopentane Amino Acid Building Blocks **19**−**22**[a]

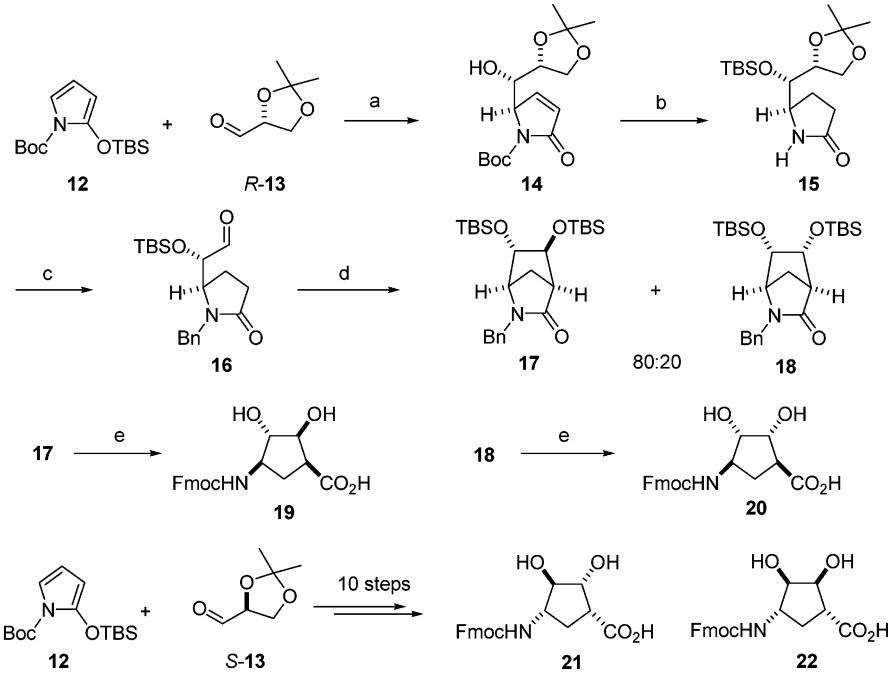

[a] Reagents: (a) $SnCl_4$, Et_2O, −90 °C (82%); (b) (i) H_2, Pd/C, EtOAc; (ii) TBSOTf, 2,6-lutidine, CH_2Cl_2; (iii) CAN, CH_3CN (87%, three steps); (c) (i) BnBr, NaH, THF; (ii) H_5IO_6, EtOAc (89%, two steps); (d) TBSOTf, DIEA, CH_2Cl_2 (98%); (e) (i) Na, liq NH_3, THF; (ii) 6 N aq HCl, 80 °C; (iii) FmocOSu, Et_3N, MeCN (89% for **19**, 67% for **20**, three steps).

1:1:3 v/v mixture of AcOH, TFE, CH_2Cl_2. The crude linear peptides were thus obtained in yields ranging from 27% to 43% for the entire solid-phase sequence. The 11 individual linear peptides were cyclized in solution (2.5 mM in DMF) at room temperature using diphenylphosphoryl azidate (DPPA) activation in the presence of solid sodium hydrogen carbonate. After chromatographic purification, the side-chain deprotection was carried out under acidic conditions in the presence of scavengers, with the reagent system TFA, phenol, H_2O, thioanisole, and 1,2-ethanedithiol (EDT). The resulting compounds were first purified by preparative reversed-phase HPLC and finally transformed into stabile hydrochloride salts by exposing the solid materials thus obtained to anhydrous HCl (gas) until a constant weight was reached. The global yields of the cyclization/deprotection step ranged from good (68−98%) for compounds **1**−**6** and **8**−**9**, carrying a cyclopentane motif with a CO/NH cis disposition, to moderate (34−70%) for compounds **7**, **10**, and **11** that bear a trans-configured amino/carbonyl cyclopentane substitution.

The purity of each macrocycle in the 11-component collection **1**−**11** was checked by two independent RP-HPLC analyses and judged to be ≥98% for all materials. The synthesis scale was in the range of 22 mg for **1** to 68 mg for **3**. All RGD macrocycles were characterized by high-resolution ESI mass spectrometry as well as various NMR techniques (see infra).

Biological Results. The ability of cyclopeptides **1**−**11** to compete with [^{125}I]-echistatin for binding to the isolated, purified $\alpha_V\beta_3$ and $\alpha_V\beta_5$ receptors was evaluated in a solid-phase receptor assay[17] and compared with

Scheme 2. Synthesis of Monohydroxylated and Dideoxycyclopentane Amino Acid Building Blocks **30**−**36**[a]

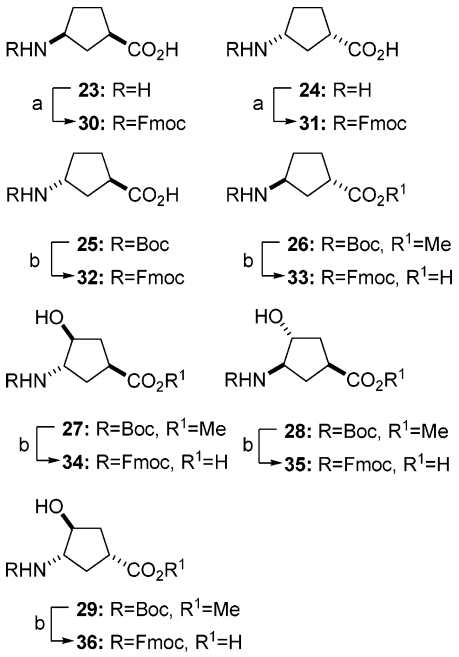

[a] Reagents: (a) FmocOSu, Et_3N, MeCN (75% for **30**, 38% for **31**); (b) (i) 6 N aq HCl, 80 °C; (ii) FmocOSu, Et_3N, MeCN (50% for **32**, 68% for **33**, 86% for **34**, 88% for **35**, 83% for **36**, two steps).

that of known standard binders, EMD121974,[14a] c(-RGDfV-),[2b] and ST1646.[3b] Integrin-coated 96-well plates were incubated with the ligand in the presence of serially diluted competing compounds. The $IC_{50} \pm SD$ values (nM) were calculated as the concentration of compound required for 50% inhibition of ligand binding, as estimated by the Allfit program, and are given in Table 1.

For this strictly related compound series, the influence of the nature of the cyclopentane scaffold grafted into the RGD residue was especially analyzed. The first trend to note in the series is that the binding affinities of the RGD ligand family embodying 4,5-dihydroxylated Acpca units are invariably reduced as compared to those of the 4-hydroxy and 4,5-dideoxy analogues (e.g., **1**−**4** vs **5**−**7**, vs **8**−**11**). This indicates that the scaffold disubstitution is not as well tolerated for both the $\alpha_V\beta_3$ and $\alpha_V\beta_5$ receptor binding. In particular, comparison of the dihydroxylated derivatives **1** and **2** to 1,3-stereochemically related monohydroxylated compound **5** and dideoxy derivative **8** shows that there is a 18−31-fold increase in activity when going from two hydroxyl groups at C4 and C5 (e.g., **1** and **2**) to one hydroxyl at C4 (e.g., **5**), whereas there is only a negligible variation when going from one hydroxyl at C4 (e.g., **5**) to no hydroxyls (e.g., **8**). A similar trend is also observed for the dihydroxylated couple **3**/**4** as compared to monohydroxylated derivative **6** and dideoxy analogue **9**. This seems to indicate that though placement of one OH-group at the C4 position of the Acpca ring only displays a marginal effect, the positioning of an extra hydroxyl substituent at C5 results in a significant decrease in binding affinity.

In addition to examination of hydroxyl substituents at the C4 and C5 positions of the cyclopentane motifs, the effect of the absolute configuration at the C1 and C3 stereocenters was evaluated. The general trends in binding affinities indicate that within the subset of dideoxy Acpca-containing ligands, the systems **9** and **10** bearing an α-located amino functionality (3*R* absolute configuration) show a higher affinity than **8** and **11** that bear the amino group β-disposed (3*S* configuration). The dihydroxylated congeners **1**−**4** were also compared, and additional support for the beneficial effect of the α stereochemistry at the C3 aminated position of the Acpca ring was found. Thus, both **3** and **4** (3*S*-configured) have significantly higher affinity than **1** and **2**, with an Acpca motif carrying β-located amino functions (3*R*-configured). One notable exception is monohydroxylated compound **7**, which shows significantly lower $\alpha_V\beta_3/\alpha_V\beta_5$ binding over the corresponding congeners **5** and **6**.

Among the best candidates, **6**, **9**, and **10**, the most distinctive compound is **10**, carrying a robust, all-carbon 1,3-trans 3α-configured (1*R*,3*R*) aminocyclopentane carboxylic moiety. In binding to $\alpha_V\beta_3$, it is 3-fold superior to **9** and 4-fold superior to **6**. For $\alpha_V\beta_5$, it is 6-fold superior to **9** and 8-fold superior to **6**. When compared to reference compounds EMD121974 and ST1646, our simplified lead compound **10** proved to be of comparable or even superior binding efficiency.

Overall, this study highlighted that in this series of ligands containing simple Acpca moieties, the vacancy at the C5 carbon along with the 3α-positioning of the amino group proved beneficial for activity, whereas the presence of a hydroxyl group at the same C5 position invariably resulted in a marked loss of binding capability of the ligands. On the other hand, the relative stereodisposition of the amino and carboxyl substituents of the Acpca motif (1,3-cis vs 1,3-trans) manifests a minor impact on the activity of the corresponding RGD ligand. Possible reasons for these findings will be discussed in the next paragraphs dealing with the solution structures and computational analysis of the selected candidates.

NMR Spectroscopy and Solution Structural Analysis. The complete chemical shift assignment of proton and carbon resonances (Supporting Information, Tables S1−S3) for **1**−**11** has been carried out for water solutions (90% H_2O/10% D_2O) using one- and two-dimensional (1D and 2D) NMR experiments, following the standard procedure described in the Experimental Section.

Six analogues from this 11-member family of $\alpha_V\beta_3/\alpha_V\beta_5$ dual binders, compounds **1**, **3**, **6**, **7**, **9**, and **10**, were selected and their NMR three-dimensional (3D) solution structures determined. These analogues differ as follows: compounds **1** and **3** possess a dihydroxylated Acpca "residue", whereas the absolute configuration of the stereocenters within the ring is opposite. Furthermore, the amino and carboxyl substituents lie in a cis disposition, with trans-located hydroxyl groups. Compounds **6** and **7** lack the C5 hydroxyl but have a 1,3-cis and a 1,3-trans orientation, respectively. The two members of the dideoxycyclopentane family, **9** and **10**, differ from each other at position C1 with 1*S* and 1*R* absolute configuration, respectively. Although all these analogues showed a dual binding ability to $\alpha_V\beta_3$ and $\alpha_V\beta_5$ receptors, their affinities vary from 132.9 and 411.5 nM for **1** to 1.5 and 0.59 nM for **10**.

Scheme 3. Synthesis of Cyclopeptides **1**−**11**[a]

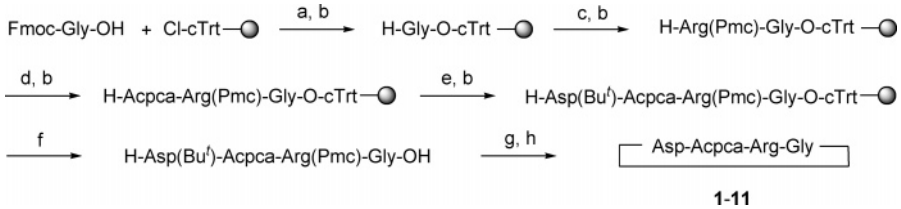

[a] Reagents: (a) DIEA, CH_2Cl_2, MeOH; (b) piperidine/DMF 20%; (c) Fmoc-Arg(Pmc)-OH, TBTU/HOBt, DIEA, NMP; (d) Fmoc-Acpca-OH, TBTU/HOBt, DIEA, NMP; (e) Fmoc-Asp(Bu^t)-OH, TBTU/HOBt, DIEA, NMP; (f) AcOH/TFE/CH_2Cl_2 (1:1:3) (27−43%, nine steps); (g) DPPA, $NaHCO_3$, DMF; (h) TFA, PhOH/H_2O/thioanisole/EDT (85.5:5:2:5:2.5) (34−98%, two steps).

Table 1. Binding Affinity of Acpca-Containing Ligands **1**−**11** in Radioligand Assays at $\alpha_V\beta_3$ and $\alpha_V\beta_5$ Integrin Receptors

cmpd	cmpd label	acpca residue[a,b]	stereochemistry	radioligand binding assay[c,d]	
				$\alpha_V\beta_3$ IC_{50} (nM)	$\alpha_V\beta_5$ IC_{50} (nM)
1	*c*[-RGDAcpca**19**-]	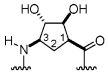	1*S*,3*R*,4*S*,5*S*	132.9±10.1	411.5±8.8
2	*c*[-RGDAcpca**20**-]	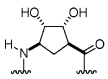	1*S*,3*R*,4*S*,5*R*	712.7±6.64	1300.0±48.7
3	*c*[-RGDAcpca**21**-]	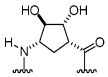	1*R*,3*S*,4*R*,5*R*	44.7±0.6	125.4±8.88
4	*c*[-RGDAcpca**22**-]	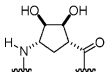	1*R*,3*S*,4*R*,5*S*	51.4±0.55	165.5±8.28
5	*c*[-RGDAcpca**35**-]	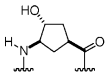	1*S*,3*R*,4*R*	7.2±0.07	13.1±0.05
6	*c*[-RGDAcpca**36**-]	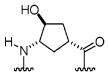	1*R*,3*S*,4*S*	5.6±0.1	4.56±0.13
7	*c*[-RGDAcpca**34**-]	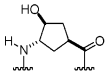	1*S*,3*S*,4*S*	35.6±0.8	29.6±0.9
8	*c*[-RGDAcpca**30**-]	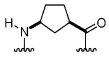	1*R*,3*S*	7.7±0.04	6.56±0.01
9	*c*[-RGDAcpca**31**-]	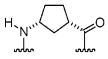	1*S*,3*R*	4.6±0.07	3.43±0.11
10	*c*[-RGDAcpca**32**-]	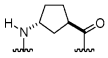	1*R*,3*R*	1.5±0.07	0.59±0.02
11	*c*[-RGDAcpca**33**-]	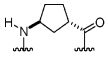	1*S*,3*S*	9.93±0.10	26.0±0.9
	EMD121974	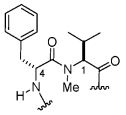	1*S*,4*R*	18.9±3.1	0.13±0.009
	c[-RGDfV-]	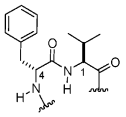	1*S*,4*R*	195.9±16.8	0.11±0.03
	ST1646	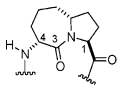	1*S*,4*R*	1.4±0.5[e]	1.16±0.2[e]
	echistatin			0.28±0.08	0.29±0.02

[a] For comparison purposes, a uniformed atom numbering for the cyclopentane residue is adopted. [b] For the reference ligands, the structure of the corresponding residue is reported. [c] Average of three or more independent determinations. [d] Compounds **1**−**11**, tested as hydrochloride salts. [e] This assay. The literature values are 3.7 ± 0.6 and 3.0 ± 0.5, respectively (ref 3b).

These analogues were selected to cover the chemical diversity of the Acpca "residues" embodied in the RGD sequence and judged sufficient for clarifying the impact that such simple cyclopentane motifs exert on the entire conformational behavior of these macrocycles as well as on their binding affinities. For the six selected compounds, the nuclear Overhauser enhancement spectroscopy (NOESY) spectra, and the $^3J_{NH-\alpha H}$ coupling constants, led to approximately 50 restraints per analogue used as input for the structure calculations (for more

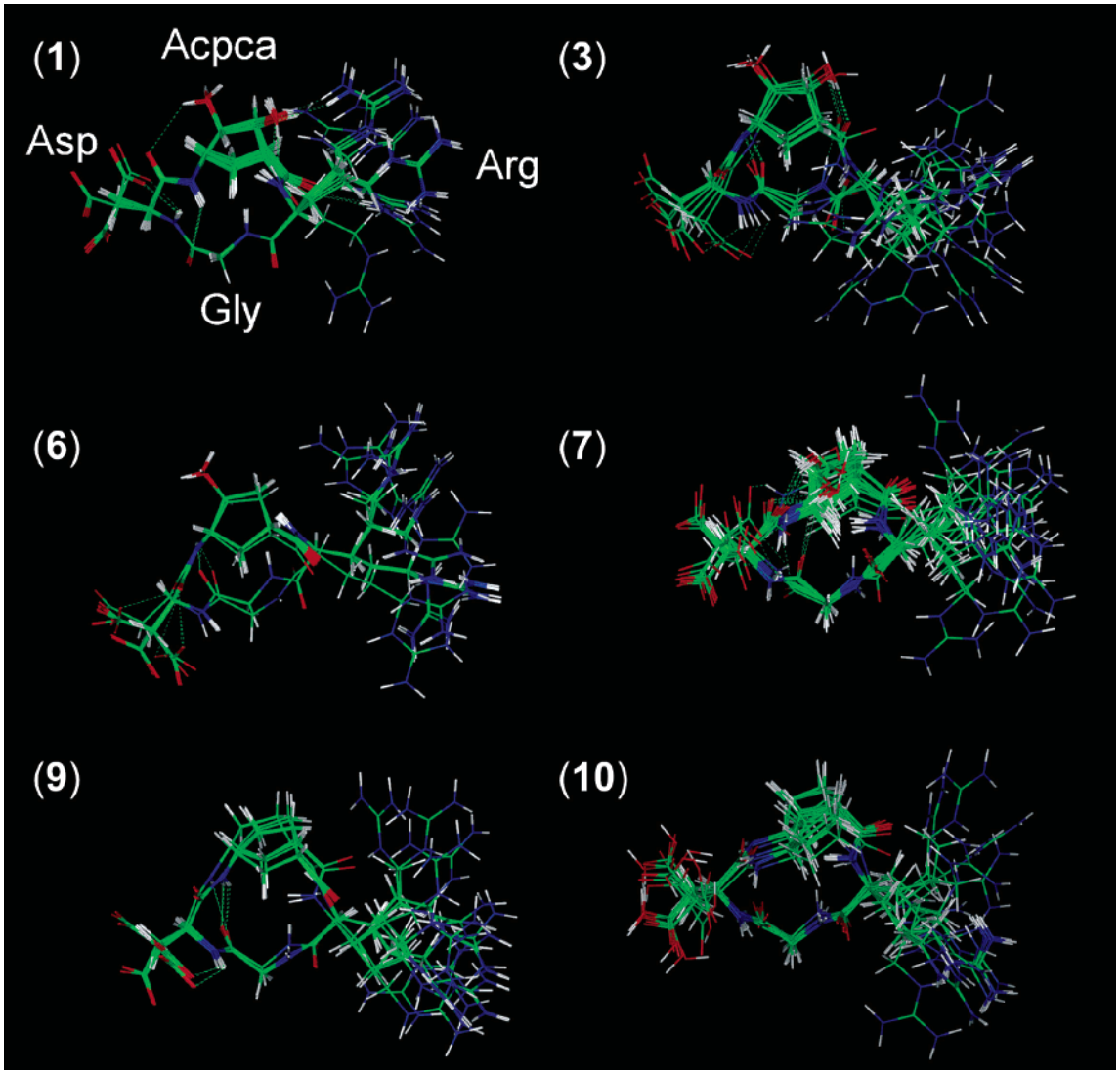

Figure 3. NMR structures of analogues **1**, **3**, **6**, **7**, **9**, and **10**. For each analogue, 20 energy-minimized conformers with the lowest energy are used to represent the 3D NMR structure. The bundle is obtained by superposing the backbone atoms of the RGD residues. The following color code is used: green − carbon; white − hydrogen; blue − nitrogen; red − oxygen. H-bonds are indicated by broken lines.

details, see the Experimental Section). Of the 100 computed structures for each compound, 20 models per analogue were selected, on the basis of the lowest-energy criterion, to represent the solution's 3D structure (Figure 3). The small residual distance violations (less than 0.3 Å) and the low dihedral angles violations (less than 3°) indicate that the input data represent a self-consistent set and the restraints are well-satisfied in the calculated conformers for each analogue.

Compound **1** binds to both receptors with low affinity (IC_{50} = 132.9 and 411.5 nM). The quality of the structure, shown in Figure 3, is reflected by the low average backbone rmsd value (0.07 Å). On the basis of the backbone torsion angle analysis (see Table S4 in Supporting Information), a family of structures (30% occurrence), characterized by an inverse γ-turn with the Asp residue in the $i+1$ position, has been identified.[23] The γ-turn motif is stabilized by a hydrogen bond (H bond) between H^N-Acpca and CO-Gly, as supported by the temperature coefficient $\Delta\delta/\Delta T = -3.5$ ppb/K experimentally observed for the amide proton of Acpca. Noteworthy, a H-bonding network responsible for the reduced flexibility of the side chains is present, that involves the Acpca C5 hydroxyl with the backbone and guanidinium moiety of Arg (50% occurrence) as well as the Acpca C4 hydroxyl with the Asp carboxylate group (23% occurrence). In addition, a significant Arg intraresidual H-bonding further reduces the flexibility of this part of the cyclopeptide. The Acpca template keeps the distance between the C^β atoms of Arg and Asp at 8.0 Å.

Analogue **3** has a 3-fold higher binding affinity than **1** and differs from it in the absolute configuration of all four stereocenters of the Acpca scaffold. The backbone torsion angles indicate that the structure contains an inverse γ-turn centered on Gly(i)-Asp($i+1$)-Acpca($i+2$) (>60% occurrence), which is highly stabilized by the presence of a H bond between the amide proton of Acpca and the carbonyl of Gly. The very low-temperature coefficient $\Delta\delta/\Delta T = -1.0$ ppb/K observed for the amide proton of Acpca, indicative of the expected H-bond AcpcaNH−COGly, along with the scarce scattering of the torsion angle values of the minimized conformers indicates a reduced conformational freedom of the macrocycle backbone as compared to that for **1**. Of the two Acpca hydroxyls at C4 and C5, only the latter is partially involved in H-bonding with the Arg side chain.

This feature results in Asp and Arg side chains experiencing an enhanced conformational freedom as compared to that of **1**, even if the distance between the C^{β} atoms of Arg and Asp is still kept at 8.0 Å by the presence of the template.

Monohydroxylated representatives **6** and **7** bind with high affinity to both integrin receptors, with the former being 6× more active than the latter. Their chemical structures differ from each other in the orientation of the carboxylic residue, cis to the amino group in **6** and trans in **7**. The calculated NMR structure of **6** possesses, again, an inverse γ-turn centered at Asp (90% populated) that is stabilized by the H bond between AcpcaNH and COGly. This is justified by the low-temperature gradient (−2.0 ppb/K) of the Acpca amide proton. As for compound **3**, no H-bonding is observed involving the C4 hydroxyl, and the Asp and Arg side chains are conformationally flexible. The C^{β} distance between Arg and Asp is 8.4 Å. In contrast, compound **7** does not present any defined secondary structures consistently with all three coupling constants $^{3}J_{NH-\alpha H}$ of ca. 7.0 Hz that suggest conformational averaging. Also, a highly populated family of conformers (51%) is present, dominated by a strong H-bond between the C4 hydroxyl and the Asp residue. Again, the distance C^{β} Asp-Arg is 8.2 Å. The comparison of compounds **6** and **7** seems to indicate that a somewhat rigid macrocycle backbone conformation associated with the absence of H-bonding involving the C4 hydroxyl represents a key element for the biological activity of **6**.

Analogues **9** and **10** are the most active compounds of this series, but the binding affinity of **10** is 3-fold higher for $\alpha_V\beta_3$ and 6-fold higher for $\alpha_V\beta_5$ than **9**. The chemical structures differ from those of compounds **1**, **3**, **6**, and **7** by the absence of hydroxyl substituents in the Acpca motifs and differ each other in the cis (**9**) vs trans (**10**) location of the Acpca scaffold substituents. The NMR data and the results of SA calculations of **9** revealed a highly rigidified and well-defined structure of the backbone, showing an inverse γ-turn with Asp in the $i+1$ position (75%). A low-temperature coefficient of −3.3 ppb/K for the amide hydrogen of Acpca is further indicative of the H-bond formation between AcpcaNH and COGly. Also, there is a consistent presence of intraresidual H-bonding of the Asp moiety, which is supported by the temperature gradient of −2.4 ppb/K for the Asp amide proton. The distance C^{β} Arg-Asp remains almost unchanged at 8.1 Å.

Strictly speaking, the NMR structure of the most active compound **10** does not evidence any classical backbone secondary structures, as indicated by the distribution of the torsion angle values and by the vicinal coupling constants $^{3}J_{NH-\alpha H}$ (ca. 7.0 Hz). However, a kinked conformation is present, populated to a degree of 90% in the 100 structures generated, centered at the Asp moiety (see Figure 3), which is also substantiated by a strong NOE contact between the Acpca NH and the αH and βH_2 Asp protons as well as by a low-temperature gradient of −2.88 ppb/K for the Acpca-amide proton. In addition, both of the side-chain residues freely rotate with no definite spatial region occupied. The C^{β} distance of Arg and Asp is 8.3 Å. Thus, a deduction can be drawn from the results involving compounds **9** and **10**; it seems that the existence of a structured cyclopeptide backbone, be it an inverse γ-turn motif or an organized kink centered at the Asp residue, associated with a great conformational freedom of the Asp and Arg pharmacophoric side chains is a stringent requisite for activity.

In summary, from the biological and structural results of this study, it can be assumed that an organized arrangement of the cyclopeptide backbone, that ensures a conformation of the macrocycle in the Arg-Gly-Asp region with C^{β} distances Asp-Arg in the range 8.0−8.4 Å, is essential for an efficient $\alpha_V\beta_3$ and $\alpha_V\beta_5$ integrin binding. Furthermore, a crucial contribution is given by the conformational freedom of the Asp and Arg side chains. When their spatial arrangement is constrained by inter- and intraresidual H-bonding as, for example, in hydroxylated compounds **1**, **3** and **7**, the binding capability is markedly eroded.

In all of the active compounds of the series, the amide proton of the Asp moiety points outward from the ring, exposed to the solvent. A remarkable exception is the worst representative of the series, dihydroxylated compound **2** (IC_{50} = 712.7 and 1300.0 nM), whose 3D NMR solution structure (data not shown) highlights a marked preference for an inverse γ-turn centered at the Gly residue. This causes the macrocycle backbone to assume a "closed" conformation with shorter C^{α} and C^{β} Asp-Arg distances (5.8 and 7.9 Å respectively). Different from the previous cases, the Asp amide proton points inside the macrocycle ring, presumably preventing the formation of crucial interactions with the binding pocket of the receptors.

Docking Studies. To understand the experimental results on a structural basis, molecular docking studies were undertaken for six representative compounds, namely dihydroxylated derivatives **1** and **3**, monohydroxylated derivatives **6** and **7**, and dideoxy derivatives **9** and **10**. The protein binding site was derived from the X-ray crystal structure of the extracellular segment of integrin $\alpha_V\beta_3$ in complex with the cyclic pentapeptide ligand EMD121974.[18b] For each analogue, representative cyclopeptide backbone conformations were selected among the energy-minimized conformers derived from the NMR data as starting structures for docking studies.

The crystal structure of the peptide/integrin complex provides the actual conformation of EMD121974 bound to the $\alpha_V\beta_3$ integrin active site and can serve as a basis for understanding the general mode of interaction of integrins with other RGD-containing ligands. Examination of the 3D structure of the cyclic pentapeptide ligand EMD121974 bound to the $\alpha_V\beta_3$ integrin receptor (Protein Data Bank entry code = 1L5G)[18b] reveals a conformation characterized by an inverse γ-turn with Asp at position ($i+1$) and by a distorted βII′-turn with Gly and Asp at the ($i+1$) and ($i+2$) positions, respectively. An 8.9 Å distance between the Asp and Arg C^{β} atoms and an almost extended conformation of the RGD sequence are observed in this pentapeptide bound conformation.

Remarkably, solution NMR-derived structures of selected Acpca-containing ligands show preferred cyclopeptide backbone arrangements featuring a γ-turn or a kink centered at the Asp residue and an extended conformation of the RGD region with average Arg-Asp C^{β} distances in the range of 8.0−8.4 Å. These geo-

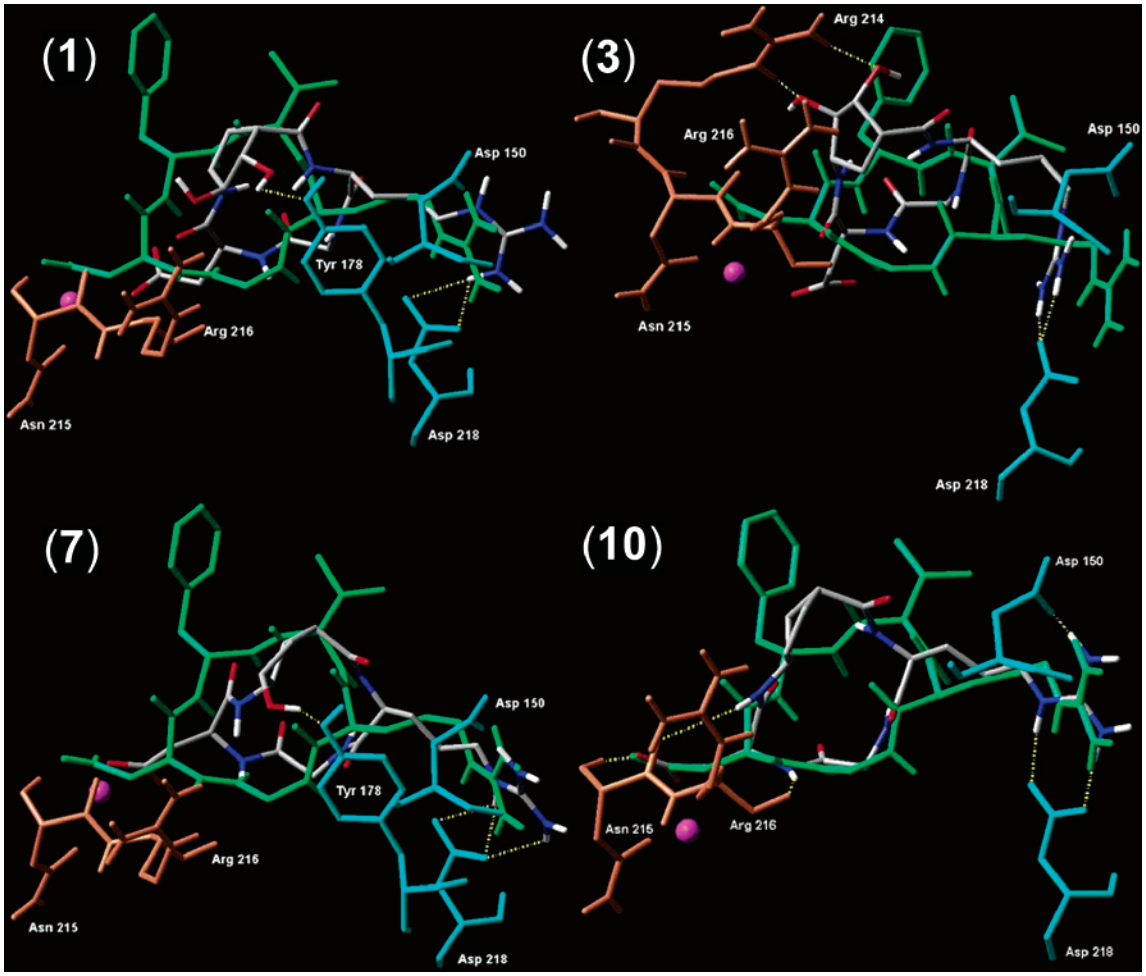

Figure 4. Results of the docking studies. Top-ranking binding modes of RGD ligands **1**, **3**, **7**, and **10** (carbon atoms are shown in gray, nitrogen atoms in blue, oxygen atoms in red, and polar hydrogen atoms in white) into the crystal structure of the extracellular domain of $\alpha_V\beta_3$ integrin overlayed on the bound conformation of EMD121974 (green). Selected integrin residues involved in the interactions with the Acpca ligands (residues of the α subunit are shown in cyan, those of the β subunit in orange) and crucial H bonds are shown. The Mn^{2+} ion at MIDAS (metal-ion-dependent adhesion site) is shown in magenta. Nonpolar hydrogens were removed for clarity.

metries are, therefore, remarkably similar to the bound EMD121974 conformation and also ensure an orientation of the Asp NH group suitable to form the H-bond ligand−receptor interactions revealed in the crystal structure.

Starting from this X-ray complex, structural models for the interactions of the selected compounds with the ligand-binding site of the $\alpha_V\beta_3$ integrin receptor were generated by automated computational docking using the Glide program[24] after removal of the peptide ligand. The obtained complexes appeared to maintain almost the same ligand−receptor distances and interactions observed in the crystalline complex of EMD121974 with $\alpha_V\beta_3$.[18b] The most important interactions involve the positively charged Arg guanidinium group of the ligand and the negatively charged side chains of Asp 150 and Asp 218 in the α subunit as well as one of the Asp carboxylate oxygens of the ligand and the metal cation in the metal-ion-dependent adhesion site (MIDAS) region of the β subunit (Figure 4). Further stabilization could occur through H bonds between the backbone NH of the Asp residue and the backbone carbonyl oxygen of Arg 216 in the β subunit as well as between the other Asp carboxylate oxygen and the backbone amide hydrogen of Asn 215 in the β subunit. Moreover, the central Gly residue is in close contact with the integrin surface. Automated docking calculations of the most active compound **10** as well as **6** and **9** (not shown in Figure 4) starting from different representative cyclopeptide backbone conformations always produced top-ranked poses conserving all these important interactions and the ligand in the same location as that for EMD121974 in the crystal structure. On the contrary, only one representative macrocycle conformation of the less active compound **7** resulted in best-score binding modes reproducing the X-ray pose. Also, the hydroxyl substituent at C4 of this monohydroxylated derivative may form a H bond with the (α) Tyr 178 OH-group, and alternative poses lacking the major interactions of the crystallographic binding geometry may occur.

Moreover, as the cleft in which the ligands bind is rather shallow, alternative binding modes differing in the orientation of the Acpca motif were found by the automated docking calculations. The guanidine and carboxy groups of the ligands seem to be essential for binding to the integrin subunits α and β, respectively, acting like an electrostatic clamp in attaching to charged regions of the protein.[25,26]

In addition to the calculated poses resembling the experimentally observed binding mode of EMD121974,

automated docking of the least active dihydroxylated derivatives **1** and **3** revealed high-score alternative binding modes differing in the H-bond pattern and in the position of the ligand within the binding pocket. In the alternative poses, the hydroxyl substituent at C5 of compound **1** forms a H bond with the (α) Tyr 178 OH-group, and both the Acpca hydroxyls at C4 and C5 of derivative **3** form H-bond interactions with the guanidinium group of the Arg 214 residue in the β subunit. As a consequence of the H bonds engaged by the functional groups of the Acpca ring, a rotation of the ligand in the binding site is observed, which prevents the formation of several important interactions disclosed by the crystal complex. Assuming that the X-ray pose describes the best interaction mode with the $\alpha_V\beta_3$ integrin receptor, this finding could explain the decrease in binding affinity observed when going from dideoxy analogues to RGD ligands containing 4,5-dihydroxylated Acpca units.[27]

In summary, the models built for the interaction of representative Acpca derivatives with $\alpha_V\beta_3$ integrin through docking studies confirmed that the macrocycle conformations of these ligands enable them to fit properly in the shallow cleft of the receptor, sharing the binding features of the crystal structure of the EMD121974−$\alpha_V\beta_3$ complex. The polar interactions and the H-bonding network governing the recognition process may be partially destroyed and modified by the Acpca scaffold substitution, frequently resulting in alternative binding modes.

Conclusions

One of the most striking features in the design of peptidomimetics is the embodiment of secondary structure-inducing scaffolds into the amino acid sequences with the perspective to force peptides into bioactive conformations and enhance stability toward degradation by enzymes.[1] In keeping with this reasoning, we synthesized 11 RGD cyclopeptides, **1**−**11**, incorporating simple, readily available aminocyclopentane carboxylic acid motifs (Acpca) and assessed their binding capabilities toward $\alpha_V\beta_3$ and $\alpha_V\beta_5$ integrin receptors. Of the compound repertoire prepared covering a wide range of binding affinities, four representatives, **6**, **8**, **9**, and **10**, displayed one-digit nanomolar dual binding levels, with analogue **10** being the best candidate (IC_{50} = 1.5 nM vs $\alpha_V\beta_3$ and 0.59 nM vs $\alpha_V\beta_5$). These values are comparable or even superior to those of several RGD-based high-affinity binders reported in the literature, including the reference compounds EMD121974, c[-RGDfV-], and ST1646.

The data from this study, supported by in-solution 3D NMR structural results and docking evidences, highlight several points: first, the nonisosteric (yet bioisosteric) substitution[15] of a cyclopentane γ-amino acid motif spanning five atoms for a six-atom dipeptidic/pseudodipeptidic spacer proved beneficial for the development of high affinity integrin binders;[28] second, a close similarity of the ligand backbone conformation was found for all the active compounds in this series, which ideally matches the receptor-bound conformation; third, the presence of hydroxyl substituents at the Acpca nucleus heavily depletes the binding affinity of the ligands for parasitic, noncooperative polar interactions and H-bonding networks involving these substituents and alternative binding sites of the receptor may occur, that prevent these ligands from fitting properly into the shallow cleft of the binding pocket.

All in all, these results establish γ-aminocyclopentane carboxylic acids, conformationally restricted GABA surrogates, as privileged scaffolds capable of generating functional molecular binders of useful peptidal secondary structures. Efforts to develop more potent integrin blocking agents and conjugates[29] embodying GABA-reminiscent pentacyclic scaffolds equipped with tunable anchoring functionalities continue in our laboratories.

Experimental Section

For routine experimental procedures and spectroscopic data, see the Supporting Information.

c[-Arg-Gly-Asp-Acpca19-] (1) (General Procedure for Cyclopeptides Synthesis). Resin Loading. All number of equivalents of reagents are given relative to the resin loading (mmol/g). In a solid-phase reaction vessel, to the cTrt resin (101 mg, 0.181 mmol) preswollen in CH_2Cl_2 (30 min), was added a solution of Fmoc-Gly-OH (135 mg, 0.453 mmol) and DIEA (72 μL, 0.416 mmol) in CH_2Cl_2 (2.5 mL). The reaction mixture was stirred under a flow of nitrogen for 1 h. After adding another 72 μL of DIEA (0.416 mmol) and 430 μL of MeOH, the mixture was shaken for a further 30 min and drained, and the resin was washed several times with DMF (3 × 3 mL), CH_2Cl_2 (5 × 3 mL), Pr^{i}OH (2 × 3 mL), MeOH (5 × 3 mL), Et_2O (2 × 3 mL), and CH_2Cl_2 (3 × 3 mL). The Fmoc-Gly resin, swollen in DMF (5 × 3 mL), was treated with 5% v/v piperidine in DMF/CH_2Cl_2 1:1 (5 mL, 5 min). The solution was drained and the resin treated with 20% v/v piperidine in DMF (5 mL × 5 min × 6 cycles). The resin was washed with DMF (3 × 3 mL), Pr^{i}OH (3 × 3 mL), Et_2O (3 × 3 mL), CH_2Cl_2 (3 × 3 mL), and DMF (2 × 3 mL), and the presence of the free amino groups was checked with the TNBS test.

Peptide Coupling. A preformed solution of Fmoc-Arg-(Pmc)-OH (300 mg, 0.453 mmol), TBTU (116 mg, 0.362 mmol), HOBt (61 mg, 0.453 mmol), and DIEA (158 μL, 0.905 mmol) in NMP (2 mL) was added to the deprotected peptidyl resin. The mixture was shaken at room temperature for 1.5 h. Reaction completion was checked with the TNBS test. The solution was drained and the resin washed several times with DMF (3 × 3 mL), Pr^{i}OH (3 × 3 mL), Et_2O (2 × 3 mL), and CH_2Cl_2 (3 × 3 mL). The resin was washed again with DMF (5 × 3 mL) and then treated with 20% v/v piperidine in DMF (5 mL × 5 min × 6 cycles). The solution was drained and the resin washed with DMF (5 × 3 mL), Pr^{i}OH (3 × 3 mL), Et_2O (2 × 3 mL), CH_2Cl_2 (2 × 3 mL), and DMF (2 × 3 mL), and the presence of the free amino groups was checked with the TNBS test.

The coupling of the **Fmoc-Acpca19-OH** (104 mg, 0.271 mmol) and Fmoc-Asp(Bu^t)-OH (186 mg, 0.453 mmol) residues was carried out under the same conditions.

Acetic Acid Cleavage. The resin-bound peptide, **H-Asp-(Bu^t)-Acpca19-Arg(Pmc)-Gly-O-cTrt**, was treated with 5 mL of a mixture of acetic acid, 2,2,2-trifluoroethanol (TFE), and CH_2Cl_2 (1:1:3) for 10 min at ambient temperature. The solution was recovered and the resin carefully washed with the above AcOH/TFE/CH_2Cl_2 mixture (2 × 5 mL × 10 min). The combined solution was coevaporated in vacuo with hexane several times, furnishing 42 mg of the linear tetrapeptide **H-Asp(Bu^t)-Acpca19-Arg(Pmc)-Gly-OH** as a white solid, used as such in the subsequent synthesis step.

Cyclization. The linear tetrapeptide, **H-Asp(Bu^t)-Acpca19-Arg(Pmc)-Gly-OH** (42 mg, 0.048 mmol) was dissolved in DMF (19 mL, 2.5 mM) under nitrogen, and the solution was cooled at 0 °C. Solid $NaHCO_3$ (20 mg, 0.24 mmol) and diphenylphosphoryl azide (DPPA, 31 μL, 0.144 mmol) were added, and the reaction mixture was stirred at ambient temperature for 36 h. After filtration of excess solid $NaHCO_3$, the mixture was diluted with water and evaporated in vacuo.

The solid residue was purified by flash chromatography (EtOAc/MeOH 8:2), furnishing the protected cyclic tetrapeptide (90%) as a glassy white solid.

Side-Chain Deprotection. The protected cyclic tetrapeptide (34 mg, 0.043 mmol) was treated with 5 mL of a solution of TFA (85.5%), phenol (5%), water (2%), thioanisole (5%), and 1,2-ethanedithiol (2.5%) at ambient temperature. After 24 h, the solvent was evaporated in vacuo and the residue dissolved in 5 mL of 50% aq AcOH. The mixture was diluted with 5 mL of Et_2O and extracted with water (3 × 5 mL). The combined aqueous layers were washed with Et_2O (3 × 3 mL) and concentrated in vacuo. The crude residue was dissolved in 5 mL of 3 N aq HCl and washed again with Et_2O (3 × 3 mL). The aqueous phase was concentrated in vacuo, furnishing the deprotected cyclic tetrapeptide, **c[-Arg-Gly-Asp-Acpca19-]** (**1**) (22 mg, quant., corresponding to an overall yield of 24%), as a hydrochloride salt.

Peptide Purification. Cyclic tetrapeptide was purified by semipreparative RP-HPLC (RP C18-10 μm, 250 mm × 10 mm) using acetonitrile (0.05% TFA) in H_2O (0.05% TFA), with a 0−25% linear gradient over 25 min. A flow rate of 5.0 mL/min was used, and detection was at 220 nm. HPLC t_R = 10.2 min. The purity of the final cyclopeptide was checked with analytical HPLC (Discovery C18-10 μm column, 250 mm × 4.6 mm) in two different solvent systems (methanol/water and acetonitrile/water) using a gradient program and found to be ≥98% pure. The HPLC sample was evaporated under vacuum and finally transformed into the hydrochloride salt by exposing the solid material to anhydrous gaseous HCl until constant weight was reached, ready for biological assay. A light white solid; $[\alpha]^{20}_D$ −10.6 (*c* 0.4, H_2O); ^1H and ^{13}C NMR: see Table S1. HRMS (ES+) $C_{18}H_{30}N_7O_8$ calcd for $[MH]^+$ 472.2156, found 472.2162.

c[-Arg-Gly-Asp-Acpca20-] (2). Resin loading: 1.8 mmol/g. Overall yield: 26% (43 mg). A white solid; $[\alpha]^{20}_D$ +27.1 (*c* 0.6, H_2O) (HCl salt); HPLC purity: ≥98%; HPLC t_R = 9.3 min; ^1H and ^{13}C NMR: see Table S1. HRMS (ES+) $C_{18}H_{30}N_7O_8$ calcd for $[MH]^+$ 472.2156, found 472.2167.

c[-Arg-Gly-Asp-Acpca21-] (3). Resin loading: 1.8 mmol/g. Overall yield: 36% (68 mg). A colorless glassy solid; $[\alpha]^{20}_D$ +13.3 (*c* 0.7, H_2O) (HCl salt); HPLC purity: ≥98%; HPLC t_R = 7.5 min; ^1H and ^{13}C NMR: see Table S1. HRMS (ES+) $C_{18}H_{30}N_7O_8$ calcd for $[MH]^+$ 472.2156, found 472.2151.

c[-Arg-Gly-Asp-Acpca22-] (4). Resin loading: 1.8 mmol/g. Overall yield: 36% (66 mg). A white solid; $[\alpha]^{20}_D$ +5.7 (*c* 0.6, H_2O) (HCl salt); HPLC purity: ≥98%; HPLC t_R = 8.6 min; ^1H and ^{13}C NMR: see Table S1. HRMS (ES+) $C_{18}H_{30}N_7O_8$ calcd for $[MH]^+$ 472.2156, found 472.2165.

c[-Arg-Gly-Asp-Acpca35-] (5). Resin loading: 1.55 mmol/g. Overall yield: 30% (35 mg). A white solid; $[\alpha]^{20}_D$ +25.2 (*c* 0.7, H_2O) (HCl salt); HPLC purity: ≥98%; HPLC t_R = 9.6 min; ^1H and ^{13}C NMR: see Table S2. HRMS (ES+) $C_{18}H_{30}N_7O_7$ calcd for $[MH]^+$ 456.2207, found 456.2218.

c[-Arg-Gly-Asp-Acpca36-] (6). Resin loading: 1.55 mmol/g. Overall yield: 37% (34 mg). A glassy solid; $[\alpha]^{20}_D$ +9.2 (*c* 0.3, H_2O) (HCl salt); HPLC purity: ≥98%; HPLC t_R = 8.5 min; ^1H and ^{13}C NMR: see Table S2. HRMS (ES+) $C_{18}H_{30}N_7O_7$ calcd for $[MH]^+$ 456.2207, found 456.2196.

c[-Arg-Gly-Asp-Acpca34-] (7). Resin loading: 1.55 mmol/g. Overall yield: 15% (24 mg). A white solid; $[\alpha]^{20}_D$ −14.7 (*c* 0.1, H_2O) (HCl salt); HPLC purity: ≥98%; HPLC t_R = 9.2 min; ^1H and ^{13}C NMR: see Table S2. HRMS (ES+) $C_{18}H_{30}N_7O_7$ calcd for $[MH]^+$ 456.2207, found 456.2193.

c[-Arg-Gly-Asp-Acpca30-] (8). Resin loading: 1.6 mmol/g. Overall yield: 25% (30 mg). A white solid; $[\alpha]^{20}_D$ +12.6 (*c* 0.5, H_2O) (HCl salt); HPLC purity: ≥98%; HPLC t_R = 11.4 min; ^1H and ^{13}C NMR: see Table S3. HRMS (ES+) $C_{18}H_{30}N_7O_6$ calcd for $[MH]^+$ 440.2258, found 440.2267.

c[-Arg-Gly-Asp-Acpca31-] (9). Resin loading: 1.6 mmol/g. Overall yield: 25% (33 mg). A light white solid; $[\alpha]^{20}_D$ +10.0 (*c* 0.7, H_2O) (HCl salt); HPLC purity: ≥98%; HPLC t_R = 11.1 min; ^1H and ^{13}C NMR: see Table S3. HRMS (ES+) $C_{18}H_{30}N_7O_6$ calcd for $[MH]^+$ 440.2258, found 440.2244.

c[-Arg-Gly-Asp-Acpca32-] (10). Resin loading: 1.6 mmol/g. Overall yield: 26% (27 mg). A glassy white solid; $[\alpha]^{20}_D$ −17.5 (*c* 0.3, H_2O) (HCl salt); HPLC purity: ≥98%; HPLC t_R = 14.5 min; ^1H and ^{13}C NMR: see Table S3. HRMS (ES+) $C_{18}H_{30}N_7O_6$ calcd for $[MH]^+$ 440.2258, found 440.2251.

c[-Arg-Gly-Asp-Acpca33-] (11). Resin loading: 1.55 mmol/g. Overall yield: 24% (24 mg). A glassy white solid; $[\alpha]^{20}_D$ −20.3 (*c* 0.04, H_2O) (HCl salt); HPLC purity: ≥98%; HPLC t_R = 11.0 min; ^1H and ^{13}C NMR: see Table S3. HRMS (ES+) $C_{18}H_{30}N_7O_6$ calcd for $[MH]^+$ 440.2258, found 440.2263.

Solid-Phase Receptor Binding Assay. The receptor binding assays were performed as described previously.[17] Purified $\alpha_V\beta_3$ and $\alpha_V\beta_5$ receptors (Chemicon International Inc., Temecula, CA) were diluted to 500 and 1000 ng/mL, respectively, in coating buffer [20 mM Tris-HCl (pH 7.4), 150 mM NaCl, 2 mM $CaCl_2$, 1 mM $MgCl_2$, and 1 mM $MnCl_2$]. An aliquot of diluted receptors (100 μL/well) was added to 96-well microtiter plates and incubated overnight at 4 °C. The coating solution was removed, and 200 μL of blocking solution (coating buffer plus 1% BSA) was added to the wells and incubated for an additional 2 h at room temperature. After incubation, the plates were rinsed three times with 200 μL of blocking−binding solution and incubated for 3 h at room temperature with 0.05 and 0.1 nM [^{125}I]-echistatin (Amersham Pharmacia) for $\alpha_V\beta_3$ and $\alpha_V\beta_5$ receptor binding assays, respectively. After incubation, the plates were sealed and counted in the γ-counter (Packard).

Sample Preparation and NMR Experiments. NMR samples of cyclopeptides **1**−**11** were prepared by dissolving 3.0−5.0 mg of the analogue in 0.6 mL of 90/10 H_2O/D_2O at pH 5.5. All experiments were recorded at 300 ± 0.5 K on a Varian Inova 600 or 800 spectrometer equipped with the triple resonance probe. The chemical shifts were referenced to the H_2O signal located at 4.754 ppm. To assign the proton resonances, conventional 2D experiments, such as DQF-COSY, TOCSY, NOESY, and ROESY were recorded. The TOCSY spectrum was acquired using an MLEV-17 spin−lock sequence[30] at a field strength of 10 kHz and an evolution time of 80 ms. NOESY experiments were carried out with mixing times of 200 and 400 ms. ROESY spectra were also collected, using a continuous wave mixing of 200 and 400 ms (3.0 kHz spin−locking field strength). For the temperature coefficients of amide protons, six 1D and 2D TOCSY experiments were acquired in a temperature range from 278 to 313 K. All 2D experiments were acquired in the phase-sensitive mode using the method of States et al.,[31] recording 512−1024 t_1 experiments with a variable number of transients of 2048 complex points for each free induction decay. The spectral width in both dimensions was typically 10 ppm. In all spectra, water suppression was achieved using the WATERGATE technique. The transmitter offset was placed at the water resonance. Prior to Fourier transformation, the time-domain data were zero-filled in both dimensions to yield 4k × 2k matrixes and apodized by a shifted-squared sine bell window function to improve resolution. When required, a fourth-order polynomial baseline correction algorithm was applied after transformation and phasing. The cross-peak intensities were measured from the NOESY spectrum with a mixing time of 200 ms. No differences were observed in the NOESY spectra with different mixing times. To relate the NOEs data with the interproton distances, the calibration was made using the distance of 1.8 Å for the well-defined geminal β-protons. The NOE intensities were classified as strong, medium, and weak, corresponding to upper bound distance constraints of 2.7, 3.5, and 5.0 Å, respectively. Lower bounds between nonbonded atoms were set to the sum of their van der Waals radii (1.8 Å). Pseudoatom corrections were added to interproton distance restraints when necessary.

Vicinal proton coupling constants $^3J_{NH-\alpha H}$ were measured from well-digitized 1D proton spectra and from DQF−COSY spectra, when in the presence of resonance overlap. The dihedral angles ϕ have been estimated from the $^3J_{NH-\alpha H}$ coupling constants using the Karplus relation.

Structure Determination. The Acpca modules in the selected ligands were built using the BIOPOLYMER module of the INSIGHTII package. The linear RGD peptides were added to the template models. All calculations were carried out on a Silicon Graphics Octane workstation using the CVFF, implemented in the DISCOVER (Accelrys, San Diego, CA) software package, together with the INSIGHTII program as graphic interface. The structures of the compounds were computed using the simulated annealing (SA) method in the NMR refine module. The simulated annealing calculations included some distinct phases. Phase 1 involved randomization of all atomic coordinates, followed by minimization of the starting structures using a quadratic potential and very low force constants for each term of the pseudoenergy function, including chiral and NOE constraints. Phase 2 involved simulated annealing with a progressive increment of the force constants up to their full values. Phase 3 involved the cooling of the molecule from 1000 to 300 K over 10 ps. At the end of this protocol, the structures were energy minimized with full CVFF (Morse and Lennard-Jones potentials, Coulombic term) by steepest descents and conjugate gradients using several thousand iterations, until the maximum derivative was less than 0.001 kcal/Å. Amide bonds were kept in the more stable trans configuration. The quality of the final structures was analyzed on the basis of the number of NOE distance violations (lower than 0.3 Å) and energy values. The 3D structures of analogues **1**, **3**, **6**, **7**, **9**, and **10** are available on request to us.

Hydrogen bonds were searched using the Measure Hbond facility of INSIGHT and were regarded as present if the following criteria were satisfied simultaneously: (1) the distance between the donor H and the acceptor O was less than 2.5 Å; (2) the angle between the heavy-atom donor, the hydrogen, and the heavy-atom acceptor (NH−O) was greater than 120°.

A family of 100 structures was calculated for all compounds, and 20 models were selected on the basis of their lowest energy to represent a possible 3D structure of the compounds.

Docking Protocol. The automated molecular docking calculations were carried out using the Glide (grid-based ligand docking with energetics) module implemented in the Schrödinger's FirstDiscovery Suite, version 2.7.[24] Any docking tool needs to combine a docking engine with a fast-scoring function. Glide uses a hierarchical series of filters to search for possible locations of the ligand in the active-site region of the receptor. The shape and properties of the receptor are represented on a grid by several different sets of fields that provide progressively more accurate scoring of the ligand poses. A pose is a complete specification of the ligand: its position and orientation. Although the protein is required to be rigid, the program allows torsional flexibility in the ligand. Conformational flexibility is handled in Glide via an extensive conformational search, augmented by a heuristic screen that rapidly eliminates conformations deemed unsuitable for binding to a receptor. During the docking process, the macrocycle backbone conformation of the ligands was held fixed, whereas the side-chain dihedral angles were free to rotate.

The refined poses are scored using Schrödinger's proprietary GlideScore scoring function. GlideScore is based on ChemScore[32] but includes a steric-clash term and adds buried polar terms devised by Schrödinger to penalize electrostatic mismatches.

For the selected Acpca-containing ligands, representative energy-minimized conformers derived from the NMR data and featuring different cyclopeptide backbone geometries were used as starting conformations.

The recently solved crystal structure of the extracellular domain of the $\alpha_V\beta_3$ integrin receptor in complex with EMD121974 and in the presence of the proadhesive ion Mn^{2+} (PDB entry code = 1L5G) was used for docking studies. Because the headgroup of $\alpha_V\beta_3$ integrin has been identified in the X-ray structure as the ligand binding region, the docking was performed only on the globular head. The protein structure was setup for docking as follows. The protein was truncated to residue sequences 41−342 for chain α and 114−347 for chain β. Because of the lack of parameters, the Mn^{2+} ions in the experimental protein structure were modeled by replacing them with Ca^{2+} ions. The protein-charged groups that were neither located in the ligand-binding pocket nor involved in salt bridges were neutralized using the Schrödinger pprep script. The hydrogens were added using the Schrödinger graphical user interface Maestro,[24] and the resulting structure was optimized using the Schrödinger impref script.

The grid-generation step requires mae input files of both ligand and active site, including hydrogen atoms. The center of the grid-enclosing box was defined by the center of the bound ligand, as described in the original PDB entry. The enclosing box dimensions, which are automatically deduced from the ligand size, fit the entire active site. For the docking step, the size of the bounding box for placing the ligand center was set to 12 Å. No further modifications were applied to the default settings. The GlideScore scoring function was used to select 30 poses for each ligand.[33]

The Glide program was initially tested for its ability to reproduce the crystallized binding geometry of EMD121974. The program was successful in reproducing the experimentally found binding mode of this compound, as it corresponds to the best-scored pose.

Acknowledgment. This work was supported by Ministero dell'Istruzione, dell'Università e della Ricerca (MIUR, COFIN 2004, and FIRB 2001). We thank Dr. Emanuela Azara for LC−MS spectrometric analyses, the Centro Interfacoltà Misure "G. Casnati" (Università di Parma), and the NMR Centre of Mill Hill at the National Institute for Medical Research, London (UK) for instrumental facilities. A doctoral fellowship to P.B. from the University of Sassari is gratefully acknowledged.

Supporting Information Available: Experimental procedures and spectroscopic data for compounds **14**−**22** and **30**−**36**, NMR data (Tables S1−S3), and copies of ^{1}H NMR spectra of cyclopeptides **1**−**11**, torsion angles of energy minimized conformers of **1**, **3**, **6**, **7**, **9**, and **10** (Table S4), as well as table of elemental analyses (Table S5) of relevant intermediary compounds. This material is available free of charge via the Internet at http://pubs.acs.org.

References

(1) (a) Giannis, A.; Kolter, T. Peptidomimetics for Receptor Ligands. Discovery, Development, and Medical Perspectives. *Angew. Chem., Int. Ed. Engl.* **1993**, *32*, 1244−1267. (b) *Advances in Amino Acid Mimetics and Peptidomimetics*; Abell, A., Ed.; JAI Press: Greenwich, 1997; Vol. 1. (c) *Advances in Amino Acid Mimetics and Peptidomimetics*; Abell, A., Ed.; JAI Press: Stanford, CT, 1999; Vol. 2. (d) Randolph, J. T.; DeGoey, D. A. Peptidomimetic Inhibitors of HIV Protease. *Curr. Top. Med. Chem.* **2004**, *4*, 1079−1095. (e) Lohof, E.; Born, M. A.; Kessler, H. In *Synthesis of Peptides and Peptidomimetics*; Goodman, M., Felix, A., Moroder, L., Toniolo, C., Eds.; Houben-Weyl Methods of Organic Chemistry, 4th ed.; Georg Thieme Verlag: Stuttgart, 2003; Vol. E22b. (f) Fairlie, D. P.; Abbenante, G.; March, D. R. Macrocyclic Peptidomimetics − Forcing Peptides into Bioactive Conformations. *Curr. Med. Chem.* **1995**, *2*, 654−686.

(2) (a) Fujii, N.; Oishi, S.; Hiramatsu, K.; Araki, T.; Ueda, S.; Tamamura, H.; Otaka, A.; Kusano, S.; Terakubo, S.; Nakashima, H.; Broach, J. A.; Trent, J. O.; Wang, Z.; Peiper, S. C. Molecular-Size Reduction of a Potent CXCR4-chemokine Antagonist using Orthogonal Combination of Conformation- and Sequence-Based Libraries. *Angew. Chem., Int. Ed.* **2003**, *42*, 3251−3253. (b) Wermuth, J.; Goodman, S. L.; Jonczyk, A.; Kessler, H. Stereoisomerism and Biological Activity of the Selective and Superactive $\alpha_V\beta_3$ Integrin Inhibitor *cyclo*(-RGDfV-) and its Retro-Inverso Peptide. *J. Am. Chem. Soc.* **1997**, *119*, 1328−1335. (c) Nikiforovich, G. V.; Kover, K. E.; Zhang, W.-J.; Marshall, G. R. Cyclopentapeptides as Flexible Conformational Templates. *J. Am. Chem. Soc.* **2000**, *122*, 3262−3273. (d) Porcelli, M.; Casu, M.; Lai, A.; Saba, G.; Pinori, M.; Cappelletti, S.; Mascagni, P. Cyclic Pentapeptides of Chiral Sequence DLDDL as Scaffold for Antagonism of G-protein Coupled Receptors: Synthesis, Activity and Conformational Analysis by NMR and Molecular Dynamics of ITF 1565 a Substance P Inhibitor. *Biopolymers* **1999**, *50*, 211−219.

(3) (a) Hanessian, S.; McNaughton-Smith, G. A Versatile Synthesis of a β-turn Peptidomimetic Scaffold: An Approach Towards a Designed Model Antagonist of the Tachykinin NK-2 Receptor. *Bioorg. Med. Chem. Lett.* **1996**, *6*, 1567−1572. (b) Belvisi, L.; Bernardi, A.; Checchia, A.; Manzoni, L.; Potenza, D.; Scolastico, C.; Castorina, M.; Capelli, A.; Giannini, G.; Carminati, P.; Pisano, C. Potent Integrin Antagonists from a Small Library of RGD-Including Cyclic Pseudopeptides. *Org. Lett.* **2001**, *3*, 1001−1004. (c) Gosselin, F.; Tourwe, D.; Ceusters, M.; Meert, T.; Heylen, L.; Jurzak, M.; Lubell, W. D. Probing Opioid Receptor−Ligand Interactions by Employment of Indolizidin-9-One Amino Acid as a Constrained Gly2-Gly3 Surrogate in a Leucine−Enkephalin Mimic. *J. Pept. Res.* **2001**, *57*, 337−344. (d) Andreu, D.; Ruiz, S.; Carreno, C.; Alsina, J.; Albericio, F.; Jiménez, M. A.; De La Figuera, N.; Herranz, R.; Garcia-Lopez, M. T.; Gonzalez-Muniz, R. IBTM-Containing Gramicidin S Analogues: Evidence for IBTM as a Suitable Type II′ β-Turn Mimetic. *J. Am. Chem. Soc.* **1997**, *119*, 10579−10586.

(4) (a) Vianello, P.; Cozzi, P.; Galvani, A.; Meroni, M.; Varasi, M.; Volpi, D.; Bandiera, T. Solid-Phase Synthesis of a Small Library of 3-Phenylthio-3-nicotinyl Propionic Acid Derivatives Acting as Antagonists of the Integrin $\alpha_V\beta_3$. *Bioorg. Med. Chem. Lett.* **2004**, *14*, 657−661. (b) Gruner, S. A. W.; Kéri, G.; Schwab, R.; Venetianer, A.; Kessler, H. Sugar Amino Acid Containing Somatostatin Analogues that Induce Apoptosis in Both Drug-Sensitive and Multidrug-Resistant Tumor Cells. *Org. Lett.* **2001**, *3*, 3723−3725. (c) Chakraborty, T. K.; Ghosh, S.; Jayaprakash, S.; Sharma, J. A. R. P.; Ravikanth, V.; Diwan, P. V.; Nagaraj, R.; Kunwar, A. C. Synthesis and Conformational Studies of Peptidomimetics Containing Furanoid Sugar Amino Acids and a Sugar Diacid. *J. Org. Chem.* **2000**, *65*, 6441−6457.

(5) Cox, D.; Aoki, T.; Seki, J.; Motoyama, Y.; Yoshida, K. The Pharmacology of the Integrins. *Med. Res. Rev.* **1994**, *14*, 195−228.

(6) (a) Ojima, I.; Chakravarty, S.; Dong, Q. Antithrombotic Agents: From RGD to Peptide Mimetics. *Bioorg. Med. Chem.* **1995**, *3*, 337−360. (b) Samanen, J. GPIIb/IIIa Antagonists. *Annu. Rep. Med. Chem.* **1996**, *31*, 91−100.

(7) (a) Marugán, J. J.; Manthey, C.; Anaclerio, B.; Lafrance, L.; Lu, T.; Markotan, T.; Leonard, K. A.; Crysler, C.; Eisennagel, S.; Dasgupta, M.; Tomczuk, B. Design, Synthesis, and Biological Evaluation of Novel Potent and Selective $\alpha_V\beta_3/\alpha_V\beta_5$ Integrin Dual Inhibitors with Improved Bioavailability. Selection of the Molecular Core. *J. Med. Chem.* **2005**, *48*, 926−934. (b) Cardo-Vila, M.; Arap, W.; Pasqualini, R. $\alpha_V\beta_5$ Integrin-Dependent Programmed Cell Death Triggered by a Peptide Mimic of Annexin V. *Mol. Cell* **2003**, *11*, 1151−1162. (c) Eskens, F. A. L. M.; Dumez, H.; Hoekstra, R.; Perschl, A.; Brindley, C.; Bottcher, S.; Wynendaele, W.; Drevs, J.; Verweij, J.; van Oosterom, A. T. Phase I and Pharmacokinetic Study of Continuous Twice Weekly Intravenous Administration of Cilengitide (EMD 121974), a Novel Inhibitor of the Integrins $\alpha_V\beta_3$ and $\alpha_V\beta_5$ in Patients with Advanced Solid Tumours. *Eur. J. Cancer* **2003**, *39*, 917−926. (d) Strömblad, S.; Cheresh, D. A. Integrins, Angiogenesis and Vascular Cell Survival. *Chem. Biol.* **1996**, *3*, 881−885. (e) Chen, X.; Plasencia, C.; Hou, Y.; Neamati, N. Synthesis and Biological Evaluation of Dimeric RGD Peptide−Paclitaxel Conjugate as a Model for Integrin-Targeted Drug Delivery. *J. Med. Chem.* **2005**, *48*, 1098−1106 (corigendum, *J. Med. Chem.* **2005**, *48*, 5874).

(8) (a) Wang, J.; Sprinter, T. A. Structural Specializations of Immunoglobulin Superfamily Members for Adhesion to Integrins and Viruses. *Immunol. Rev.* **1998**, *163*, 197−215. (b) Shimizu, Y.; Rose, D. M.; Ginsberg, M. H. Integrins in the Immune System. *Adv. Immunol.* **1999**, *72*, 325−380.

(9) (a) Danen, E. H. J. Integrins: Regulators of Tissue Function and Cancer Progression. *Curr. Pharm. Des.* **2005**, *11*, 881−891. (b) Yun, Z.; Menter, D. G.; Nicolson, G. L. Involvment of Integrin $\alpha_V\beta_3$ in Cell Adhesion, Motility, and Liver Metastasis of Murine RAW117 Large Cell Lymphoma. *Cancer Res.* **1996**, *56*, 3103−3111.

(10) (a) Duong, L. T.; Rodan, G. A. Regulation of Osteoclast Formation and Function. *Rev. Endocr. Metab. Disord.* **2001**, *2*, 95−104. (b) Robey, P. G. RGD-Containing Proteins and Bone. *Annu. Rep. Med. Chem.* **1993**, *28*, 227−236. (c) Engleman, V. W.; Nickols, G. A.; Ross, F. P.; Horton, M. A.; Griggs, D. W.; Settle, S. L.; Ruminski, P. G.; Teitelbaum, S. L. A Peptidomimetic Antagonist of the $\alpha_V\beta_3$ Integrin Inhibits Bone Resorption in vitro and Prevents Osteoporosis in vivo. *J. Clin. Invest.* **1997**, *99*, 2284−2292.

(11) (a) Matsuno, H.; Stassen, J. M.; Vermylen, J.; Deckmyn, H. Inhibition of Integrin Function by a Cyclic RGD-Containing Peptide Prevents Neointima Formation. *Circulation* **1994**, *90*, 2203−2206. (b) Choi, E. T.; Engel, L.; Callow, A. D.; Sun, S.; Trachtenberg, J.; Santoro, S.; Ryan, U. S. Inhibition of Neointimal Hyperplasia by Blocking $\alpha_V\beta_3$ Integrin with a Small Peptide Antagonist GpenGRGDSPCA. *J. Vasc. Surg.* **1994**, *19*, 125−134.

(12) Bazan-Socha, S.; Bukiej, A.; Marcinkiewicz, C.; Musial, J. Integrins in Pulmonary Inflammatory Diseases. *Curr. Pharm. Des.* **2005**, *11*, 893−901.

(13) (a) Pytela, R.; Pierschbacher, M. D.; Argraves, S.; Suzuki, S.; Ruoslahti, E. Arginine-Glycine-Aspartic Acid Adhesion Receptors. *Methods Enzymol.* **1987**, *144*, 475−489. (b) Goodman, S. L.; Holzemann, G.; Sulyok, G. A. G.; Kessler, H. Nanomolar Small Molecule Inhibitors for $\alpha_V\beta_6$, $\alpha_V\beta_5$, and $\alpha_V\beta_3$ Integrins. *J. Med. Chem.* **2002**, *45*, 1045−1051.

(14) (a) Dechantsreiter, M. A.; Planker, E.; Mathä, B.; Lohof, E.; Hölzemann, G.; Jonczyk, A.; Goodman, S. L.; Kessler, H. *N*-Methylated Cyclic RGD Peptides as Highly Active and Selective $\alpha_V\beta_3$ Integrin Antagonists. *J. Med. Chem.* **1999**, *42*, 3033−3040. (b) Belvisi, L.; Caporale, A.; Colombo, M.; Manzoni, L.; Potenza, D.; Scolastico, C.; Castorina, M.; Cati, M.; Giannini, G.; Pisano, C. Cyclic RGD Peptides Containing Azabicycloalkane Reverse-Turn Mimics. *Helv. Chim. Acta* **2002**, *85*, 4353−4368. (c) Haubner, R.; Schmitt, W.; Hölzemann, G.; Goodman, S. L.; Jonczyk, A.; Kessler, H. Cyclic RGD Peptides Containing β-Turn Mimetics. *J. Am. Chem. Soc.* **1996**, *118*, 7881−7891. (d) Lohof, E.; Planker, E.; Mang, C.; Burkhart, F.; Dechantsreiter, M. A.; Haubner, R.; Wester, H. J.; Schwaiger, M.; Hölzemann, G.; Goodman, S. L.; Kessler, H. Carbohydrate Derivatives for Use in Drug Design: Cyclic α_V-Selective RGD Peptides. *Angew. Chem., Int. Ed.* **2000**, *39*, 2761−2764.

(15) (a) Thornber, C. W. Isosterism and Molecular Modification in Drug Design. *Chem. Soc. Rev.* **1979**, *8*, 563−580. (b) Chen, X.; Wang, W. The Use of Bioisosteric Groups in Lead Optimization. In *Annual Reports in Medicinal Chemistry*; Doherty, A. M., Ed.; Elsevier Academic Press: Amsterdam, 2003; Vol. 38, pp 333−346.

(16) For recent examples of nonisosteric replacement in RGD-containing cyclic ligands, see: (a) van Well, R. M.; Overkleeft, H. S.; van der Marel, G: A.; Bruss, D.; Thibault, G.; de Groot, P. G.; van Boom, J. H.; Overhand, M. Solid-Phase Synthesis of Cyclic RGD-Furanoid Sugar Amino Acid Peptides as Integrin Inhibitors. *Bioorg. Med. Chem. Lett.* **2003**, *13*, 331−334. (b) Royo, M.; Van Den Nest, W.; del Fresno, M.; Frieden, A.; Yahalom, D.; Rosenblatt, M.; Chorev, M.; Albericio, F. Solid-Phase Syntheses of Constrained RGD Scaffolds and Their Binding to the $\alpha_V\beta_3$ Integrin Receptor. *Tetrahedron Lett.* **2001**, *42*, 7387−7391. (c) Schumann, F.; Müller, A.; Koksch, M.; Müller, G.; Sewald, N. Are β-Amino Acids γ-Turn Mimetics? Exploring a New Design Principle for Bioactive Cyclopeptides. *J. Am. Chem. Soc.* **2000**, *122*, 12009−12010. (d) Annis, D. A.; Helluin, O.; Jacobsen, E. N. Stereochemistry as a Diversity Element: Solid-Phase Synthesis of Cyclic RGD Peptide Derivatives by Asymmetric Catalysis. *Angew. Chem., Int. Ed.* **1998**, *37*, 1907−1909.

(17) Kumar, C. C.; Nie, H.; Rogers, C. P.; Malkowski, M.; Maxwell, E.; Catino, J. J.; Armstrong, L. Biochemical Characterization of the Binding of Echistatin to Integrin $\alpha_V\beta_3$ Receptor. *J. Pharmacol. Exp. Ther.* **1997**, *283*, 843−853.

(18) (a) Xiong, J.-P.; Stehle, T.; Diefenbach, B.; Zhang, R.; Dunker, R.; Scott, D. L.; Joachimiak, A.; Goodman, S. L.; Arnaout, M. A. Crystal Structure of the Extracellular Segment of Integrin $\alpha_V\beta_3$. *Science* **2001**, *294*, 339−345. (b) Xiong, J.-P.; Stehle, T.; Zhang, R.; Joachimiak, A.; Frech, M.; Goodman, S. L.; Arnaout, M. A. Crystal Structure of the Extracellular Segment of Integrin $\alpha_V\beta_3$ in Complex with an Arg-Gly-Asp Ligand. *Science* **2002**, *296*, 151−155.

(19) Rassu, G.; Auzzas, L.; Pinna, L.; Zambrano, V.; Zanardi, F.; Battistini, L.; Marzocchi, L.; Acquotti, D.; Casiraghi, G. Variable Strategy toward Carbasugars and Relatives. 4. Viable Access to (4a-Carbapentofuranosyl)amines, (5a-Carbahexopyranosyl)-amines, and Amino Acids Thereof. *J. Org. Chem.* **2002**, *67*, 5338−5342.

(20) Wu, W.-L.; Wu, Y.-L. Chemoselective Hydrolysis of Terminal Isopropylidene Acetals and Subsequent Glycol Cleavage by Periodic Acid in One Pot. *J. Org. Chem.* **1993**, *58*, 3586−3588.

(21) For previous syntheses of 3-aminocyclopentane carboxylic acids see, for example: (a) Nakamura, S.; Karasawa, K.; Tanaka, N.; Yonehara, H.; Umezawa, H. Structure of Amidinomycin. *J. Antibiot. Ser. A* **1960**, *13*, 362−365. (b) Allan, R. D.; Johnston, G. A. R.; Twitchin, B. Synthesis of Analogues of GABA. III. All Four Stereoisomers of 3-Aminocyclopentanecarboxylic Acid and a Stereochemical Correlation with Amidinomycin. *Aust. J. Chem.* **1979**, *32*, 2517−2521. (c) Evans, C.; McCague, R.; Roberts, S. M.; Sutherland, A. G. Synthesis of Either Enantiomer of *cis*-3-Aminocyclopentanecarboxylic Acid from Both Enantiomers of Racemic 2-azabicyclo[2.2.1]hept-5-en-3-one. *J. Chem. Soc., Perkin Trans. 1* **1991**, 656−657. (d) Chênevert, R.; Martin, R. Enantioselective Synthesis of (+) and (−)-*cis*-3-Aminocyclopentanecarboxylic Acids by Enzymatic Asymmetrization. *Tetrahedron: Asymmetry* **1992**, *3*, 199−200.

(22) Blankenstein, J.; Zhu, J. Conformation-Directed Macrocyclization Reactions. *Eur. J. Org. Chem.* **2005**, 1949−1964.

(23) Herrero, S.; García-López, M. T.; Latorre, M.; Cenarruzabeitia, E.; Del Río, J.; Herranz, R. 2-Oxopiperazine-Based γ-Turn Conformationally Constrained Peptides: Synthesis of CCK-4 Analogues. *J. Org. Chem.* **2002**, *67*, 3866−3873.
(24) Schrödinger, http://www.schrodinger.com
(25) Gottschalk, K.-E.; Kessler, H. The Structures of Integrins and Integrin−Ligand Complexes: Implications for Drug Design and Signal Transduction. *Angew. Chem., Int. Ed.* **2002**, *41*, 3767−3774.
(26) Marinelli, L.; Lavecchia, A.; Gottschalk, K.-E.; Novellino, E.; Kessler, H. Docking Studies on $\alpha_v\beta_3$ Integrin Ligands: Pharmacophore Refinement and Implications for Drug Design. *J. Med. Chem*. **2003**, *46*, 4393−4404.
(27) The hydrophobicity of the peptidomimetic scaffold grafted into cyclic RGD ligands could affect the binding affinity to the integrin receptors (see ref 25). Lowering the hydrophobic character of the ligands by hydroxyl substituents could render dihydroxy analogues in this series less active than the nonhydroxylated counterparts. We thank the reviewers for drawing this point to our attention.
(28) Similar ring contractions in cyclopeptide constructs were recently reported: (a) Sukopp, M.; Schwab, R.; Marinelli, L.; Biron, E.; Heller, M.; Várkondi, E.; Pap, Á.; Novellino, E.; Kéri, G.; Kessler, H. Structure−Activity Relationship Studies Optimizing the Antiproliferative Activity of Novel Cyclic Somatostatin Analogues Containing a Restrained Cyclic β-Amino Acid. *J. Med. Chem.* **2005**, *48*, 2916−2926. (b) Tamamura, H.; Araki, T.; Ueda, S.; Wang, Z.; Oishi, S.; Esaka, A.; Trent, J. O.; Nakashima, H.; Yamamoto, N.; Peiper, S. C.; Otaka, A.; Fujii, N. Identification of Novel Low Molecular Weight CXCR4 Antagonists by Structural Tuning of Cyclic Tetrapeptide Scaffolds. *J. Med. Chem.* **2005**, *48*, 3280−3289.
(29) For a recent example of RGD peptide−paclitaxel conjugate, see ref 7e.
(30) (a) Davis, D. G.; Bax, A. Assignment of Complex ^{1}H NMR Spectra via Two-Dimensional Homonuclear Hartmann−Hahn Spectroscopy. *J. Am. Chem. Soc.* **1985**, *107*, 2820−2821. (b) Bax, A.; Davis, D. G. MLEV-17-Based Two-Dimensional Transverse NOE Spectroscopy. *J. Magn. Reson.* **1985**, *63*, 207−213.
(31) States, D. J.; Haberkorn, R. A.; Ruben, D. J. A Two-Dimensional Nuclear Overhauser Experiment with Pure Absorption Phase in Four Quadrants. *J. Magn. Reson.* **1982**, *48*, 286−292.
(32) Eldridge, M. D.; Murray, C. W.; Auton, T. R.; Paolini, G. V.; Mee, R. P. Empirical Scoring Functions. 1. The Development of a Fast Empirical Scoring Function to Estimate the Binding Affinity of Ligands in Receptor Complexes. *J. Comput.-Aided Mol. Des.* **1997**, *11*, 425−445.
(33) Kellenberger, E.; Rodrigo, J.; Muller, P.; Rognan, D. Comparative Evaluation of Eight Docking Tools for Docking and Virtual Screening Accuracy. *Proteins: Struct., Funct., Bioinf.* **2004**, *57*, 225−242.

JM050698X